Journal of Alloys and Compounds 509 (2011) 929–935

Contents lists available at ScienceDirect

Journal of Alloys and Compounds

journal homepage: www.elsevier.com/locate/jallcom

Sn_xS_y compounds growth by controlled sulfurisation of SnO_2

C. Khelia, K. Boubaker, M. Amlouk*

Equipe de Physique des dispositifs à Semiconducteurs, Faculté des Sciences de Tunis, Campus Universitaire, 2092 Tunis, Tunisia

ARTICLE INFO

Article history:
Received 12 July 2010
Received in revised form
22 September 2010
Accepted 22 September 2010
Available online 7 October 2010

PACS:
73.61.Le
78.66.Li
79.60.Dp
61.10.Nz
68.55.Jk

Keywords:
Sn_xS_y
Thin film
Amlouk–Boubaker opto-thermal expansivity ψ_{AB}
Optical properties
Sulfurisation
Boubaker Polynomials Expansion Scheme
BPES

ABSTRACT

In this work, thin layers of semiconducting tin sulfide Sn_xS_y compounds have been prepared by sulfrisation of tin oxide SnO_2 on glass substrate. Structural studies showed that, depending on sulfur supply concentration, a mixture of SnS_2 and Sn_2S_3 is obtained at an annealing temperature of 550 °C for 2 h. From the transmission and reflectance spectra, the extinction coefficient and refractive index were calculated as guides to understanding crystal growth kinetics. On the other hand, the exploitation of these optical measurements along with optothermal investigations showed that the electronic transitions in these layers were of allowed direct type and exhibit two gaps indicating the presence of two competent sulfide phases: SnS_2 and Sn_2S_3.

1. Introduction

Tin sulfide Sn_xS_y is a chalcogenide compound which belongs to a family of IV–VI semiconductors that have attracted attention in recent decades due to its numerous applications. Its band gap energy, varying within in the range of 0.8–3.5 eV [1,2] makes it suitable as an absorber or window layers in photovoltaic solar cells due to the possibility of the change of its character n- [3,4] or p-type [5]. Moreover, thin films of this compound, which contain no toxic constituents, have been prepared using different methods such as: vacuum evaporation [6], chemical deposition [7], electrodepostion [8], physical vapor transport [5], dip deposition [9], spray pyrolysis [10–12], chemical vapor transport [13–15] molecular beam epitaxy [16] SILAR [17,18], chemical vapor deposition [19] and PECVD [20].

In this work, Sn_xS_y thin films have been prepared by sulfurisation of fluorine-doped tin oxide SnO_2. Precursor materials have been obtained using a low-cost spray pyrolysis technique, while sulfurisation process was achieved under vacuum inside a controlled sulfurised medium. The structural and optical properties of the as-grown layers have been investigated in the cases of light and heavy sulfur content. A particular attention has been given to the oxygen–sulfur substitution kinetics during layer growth as well as the variety of the obtained compounds.

2. Experimental details

2.1. Films growth

First, fluorine-doped tin oxide SnO_2:F thin film was prepared on glass substrate by the spray pyrolysis technique using tin tetrachloride ($SnCl_4$) methanol distilled water and ammonium fluorine as starting materials. The solution and gas flow rates were maintained at 1.5 L min^{-1} and 4 L min^{-1}, respectively corresponding to a mini-spray pyrolysis. The Pyrex substrates prepared in 20 mm × 10 mm × 3 mm dimensions were cleaned in advance in a boiling solution of chromic acid, deionized water and ultrasonic bath. The cooled substrates were placed on a heater sink which temperature T_s was maintained at 440 °C [21]. The precursor solution was sprayed through a preheating furnace on Plexiglas substrates. Nitrogen (N_2) was used as carrier gas. The chemical process leading to an adherent SnO_2:F film consists of two steps:

Step A.1: The droplets of penta-hydrated stannic tetrachloride ($SnCl_4{\cdot}5H_2O$) are dissociated under the effect of the spray:

$$(SnCl_4, 5H_2O)_n + 2nH_2O \xrightarrow[\text{Carrier gas}]{\text{Spray}} n\underline{SnCl_4} + 12n\overrightarrow{H_2O} \quad \text{(Step A.1)}$$

* Corresponding author.
E-mail addresses: math_physics2008@yahoo.fr, mmbb11112000@yahoo.fr (M. Amlouk).

0925-8388/$ – see front matter © 2010 Elsevier B.V. All rights reserved.
doi:10.1016/j.jallcom.2010.09.132

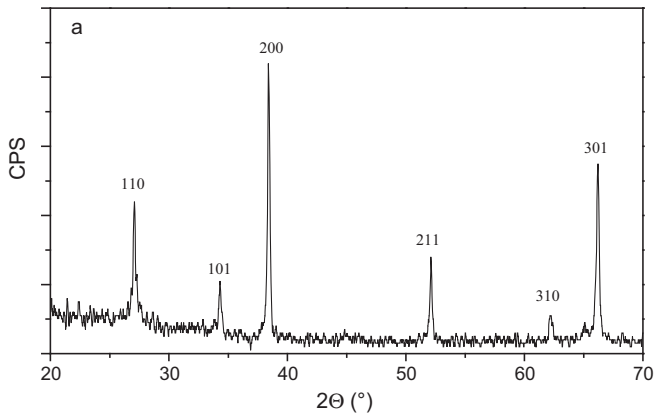

Fig. 1. X-ray diffraction of SnO_2:F (e = 1.2 μm).

Step A.2: The ammonium florid acts on the deposited (and heated) stannic tetrachloride according to an incorporation process due to ionic close electro-negativity and dimension (the radii ratio of the ions F^- and O^{2-} is around 0.96). Emanations of di-hydrogen and ammoniac gases have been verified experimentally.

$$n\,SnCl_4 + n(NH_4^+, F^-) + 2n\,H_2O \xrightarrow[methanol]{440°C} n\,SnO_2{:}F + 4n\,\overrightarrow{HCl} + n\,\overrightarrow{NH_3} + \frac{n}{2}\,\overrightarrow{H_2} \quad \text{(Step A.2)}$$

Second, the obtained SnO_2:F thin films were introduced with sulfur grains (mass = m_{grain}, 99.98% of purity) into Pyrex tubes under two conditions: (i) light sulfuring ($m_{grain} \approx 16$ mg); (ii) heavy sulfuring ($m_{grain} \approx 850$ mg). Each tube was sealed under vacuum (10^{-2}–10^{-3} Pa) and annealed during 2 h at 550 °C using a programmed tubular oven.

2.2. Characterization techniques

X-ray diffraction spectra were obtained by means of Bruker-Axs type diffractometer using two monochromatic radiations CuK_α (λ_1 = 1.54056 Å; λ_2 = 1.54438 Å). Film surfaces were analyzed by Atomic Force Microscopy (AFM: Nanoscope 3A dimension 3100 digital). Optical transmittance and reflectance measurements were carried out in the wavelength range 300–1800 nm using unpolarized light by means of a spectrophotometer (Shimadsu UV 3100 F). An integrating sphere (LISR 3200) coupled to the spectrophotometer was used for these measurements. Finally, the optothermal expansivity of each sample has been calculated through the BPES.

3. Results and discussion

3.1. X-ray diffraction investigations

XRD patterns of the deposited SnO_2:F thin films prepared at 440 °C are shown in Fig. 1.

The diffraction patterns show (1 1 0), (1 0 1), (2 0 0), (2 1 1), (3 1 0) and (3 0 1) X-ray diffraction lines which are characteristic to SnO_2 variety (JCPDS Card No. 41-1445) crystallizing in tetragonal system [22] with a little shift to the higher 2θ angles due to the fluorine doping. On the other hand, the grain size in accordance with the Scherrer–Debye formula [23] was evaluated to be 443 Å.

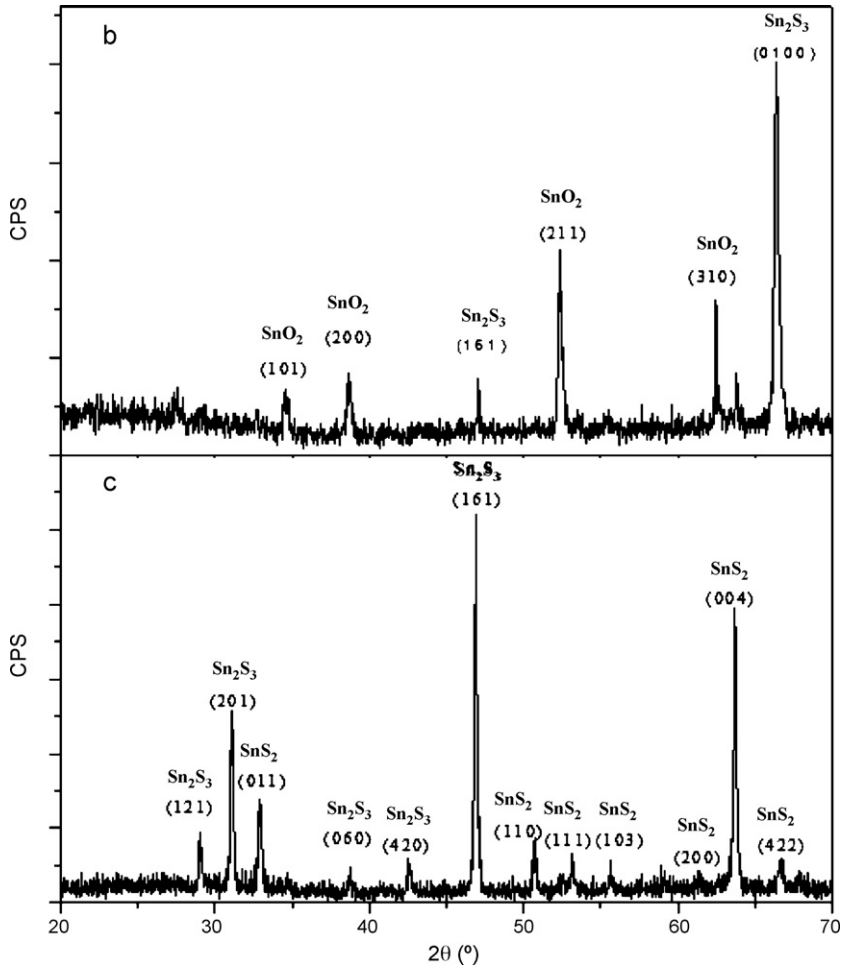

Fig. 2. X-ray diffraction of sulfured SnO_2:F (e = 1.2 μm). (b) Lightly sulfured and (c) heavily sulfured.

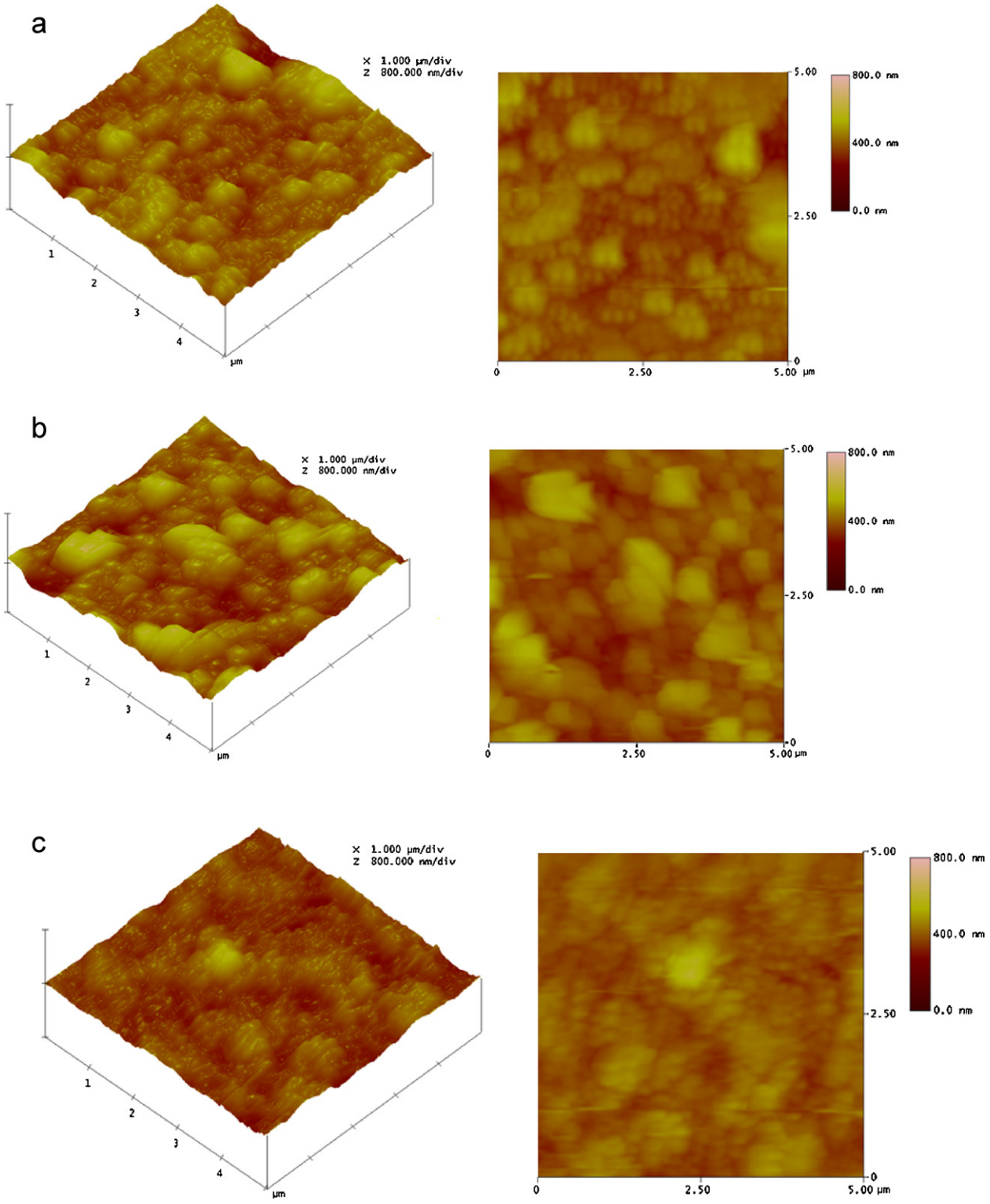

Fig. 3. 2D and 3D AFM micrographics of SnO_2:F (e = 1.2 µm). (a) Unsulfured; (b) lightly sulfured; (c) heavily sulfured.

Fig. 2 shows that annealed SnO_2 films with excess of sulfur led to the films having a mixture of two sulfide phases: SnS_2 (JCPDS: 23-677) and Sn_2S_3 (JCPDS: 30-1377) whereas whose without excess were formed by both oxide and sulfide ones. Explanation to these evolutions is detailed in the following parts.

3.2. AFM analysis

2D and 3D AFM micrographs of SnO_2:F thin film with thickness of the order of 1.2 µm (Fig. 3a) reveal that the surface of the film is perturbed by clusters with a mean dimension of 231 nm. This is due to growth mechanism of the film prepared by the spray pyrolysis

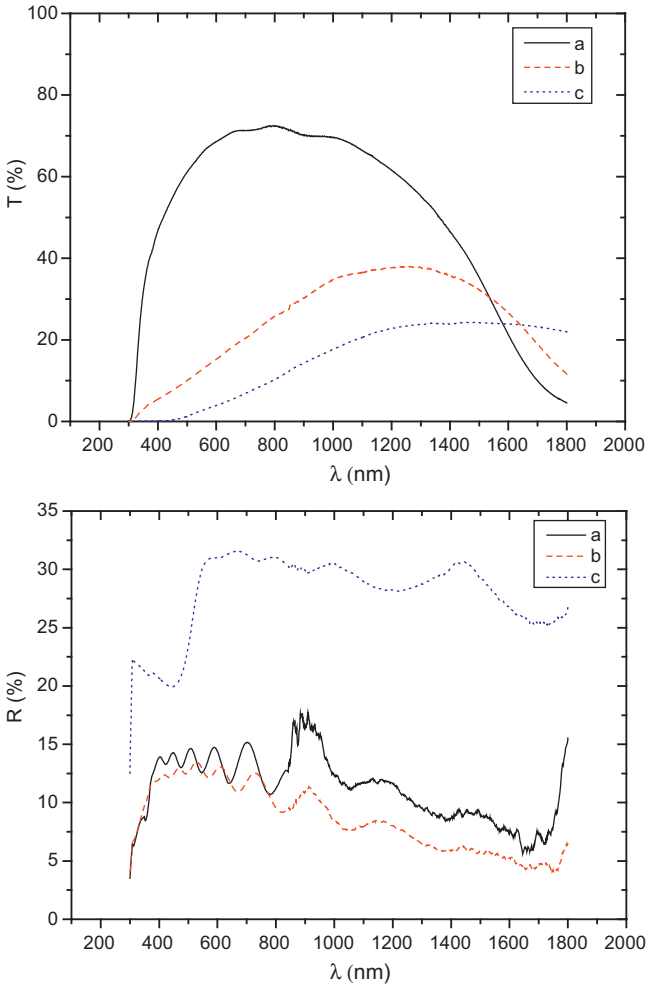

Fig. 4. Optical transmittance and reflectance spectra of SnO_2:F. (a) Unsulfured; (b) lightly sulfured; (c) heavily sulfured.

technique [24]. Indeed, the surface of the film is formed by small droplets that vaporize above the substrate and condense as microcrystallines with various dimensions. These microcrystallines then coalesce to form clusters. The mean roughness is depicted to be 44 nm. In the same way, roughness and grain size, as deduced from AFM images, showed a roughness increases at the beginning of the sulfurisation phase (58 nm) due to sulfur diffusion (bright zones in Fig. 3b). But once this latter becomes in excess, the roughness decreases (41 nm) and the surface contrast between unsulfured and sulfured zones disappears.

3.3. Optical properties

Optical transmittance and reflectance spectra in 300–1800 nm wavelength range for the SnO_2:F before and after sulfurisation of thin films are shown in Fig. 4. We note therefore that spectrum presented interferential fringes due to multiple reflections indicating that the films are relatively homogenous. These fringes became weak with sulfuring. In addition, we remarked that for SnO_2:F, the transparency was of the order of 75% and decreased with sulfuring. The decrease in the infrared was probably due to the contribution of free carriers. Considering optical reflectance measurements [25] and SEM observation, the thickness of these films was of the order of 1.2 μm.

The calculation of the extinction coefficient k and the refractive index n are made by maple program through resolving the system

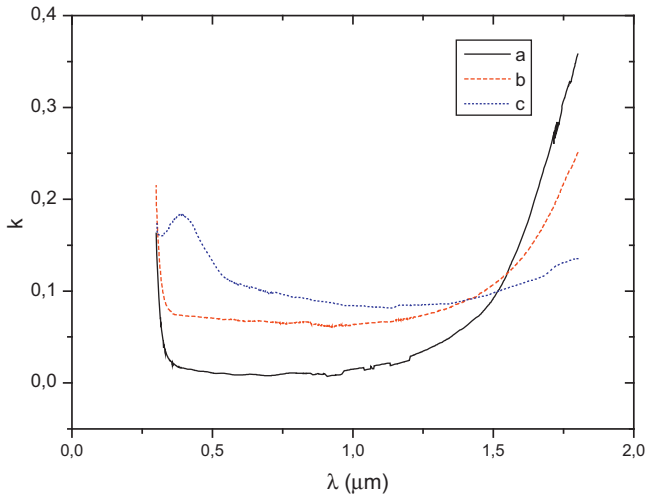

Fig. 5. Extinction coefficient spectrum. (a) Unsulfured; (b) lightly sulfured; (c) heavily sulfured.

(1) of non linear equations for each wavelength:

$$\begin{cases} R_{theor.}(n,k,\lambda) - R_{experim.}(n,k,\lambda) = 0 \\ T_{theor.}(n,k,\lambda) - T_{experim.}(n,k,\lambda) = 0 \end{cases} \quad (1)$$

where $R_{theor.}(\lambda)$ and $T_{theor.}(\lambda)$ are respectively the reflection and transmission expressions reported elsewhere [25]. The results are reported on spectrum of Figs. 5 and 6.

For all spectra, we could remark an increase of the extinction coefficient and a decrease of refraction index in the infra-red zone due to free carriers. In addition, k became higher (0.1 instead of 0.025) when film was heavily sulfured thus the film is more absorptive. Moreover a sulfur excess made refractive index higher particularly in the visible zone. This phenomenon is may be due to the sulfur engagement.

The lack of transparency traduced by increasing values of the extinction coefficient k for increasing sulfur content was in concordance with the diminution of transmittance (Fig. 4a). In the same way, the evolution of the refraction index peak (from 1.8 to 2.1 to 2.5) with increasing sulfur content revealed establishment of defects probably due to remaining atomic non-reactant sulfur.

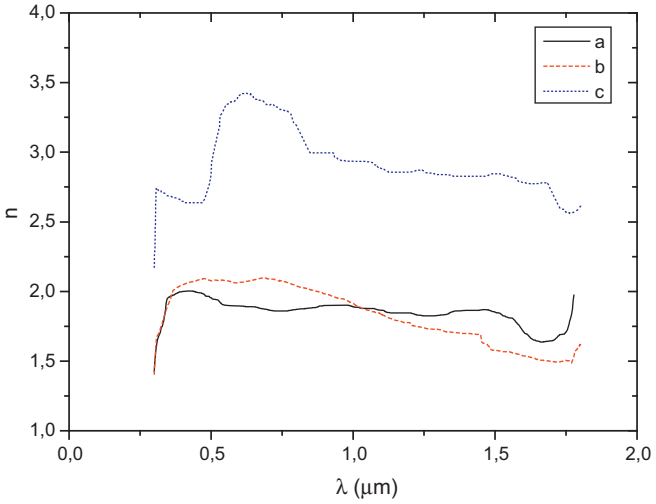

Fig. 6. Refractive index spectrum of SnO_2:F. (a) Unsulfured; (b) lightly sulfured; (c) heavily sulfured.

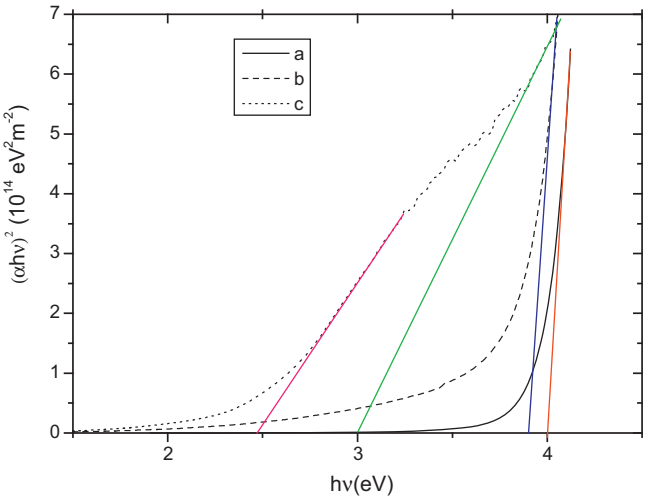

Fig. 7. $(\alpha h\nu)^2$ versus $h\nu$ plot of SnO_2:F. (a) Unsulfured; (b) lightly sulfured; (c) heavily sulfured.

The optical absorption coefficient α was deduced from the following formula:

$$\alpha = \frac{4\pi}{\lambda}k$$

Using α calculated values, the band gap energy E_g corresponding to direct band gap transitions is calculated via the $(\alpha h\nu)^2$ versus $h\nu$ plots (Fig. 7) using the formula [26]:

$$(\alpha h\nu)^2 = A(h\nu - E_g); \quad A = \text{cst.}$$

E_g values are reported along with other characteristics in Table 1.

We note that the plot corresponding to excess sulfured SnO_2:F exhibits two E_g value corresponding to two sulfur phases. These values of E_g are next to those of Sn_2S_3 and SnS_2 reported in literature [27,28]. The little difference is probably due to the presence of the remaining SnO_2 phase.

3.4. Opto-thermal study

3.4.1. Effective absorptivity $\hat{\alpha}$ and Amlouk–Boubaker opto-thermal expansivity ψ_{AB}

The effective absorptivity $\hat{\alpha}$, as defined in precedent studies [29,30], is the mean normalised absorbance weighted by $I(\tilde{\lambda})_{AM1.5}$, the solar standard irradiance:

$$\hat{\alpha} = \frac{\int_0^1 I(\tilde{\lambda})_{AM1.5} \times \alpha(\tilde{\lambda})\, d\tilde{\lambda}}{\int_0^1 I(\tilde{\lambda})_{AM1.5}\, d\tilde{\lambda}} \tag{2}$$

where $I(\tilde{\lambda})_{AM1.5}$ is the Reference Solar Spectral Irradiance, fitted using the Boubaker Polynomials Expansion Scheme (BPES) [31–39]: $I(\tilde{\lambda}) = \left[(1/2N_0)\sum_{n=1}^{N_0}\theta_n.B_{4n}(\tilde{\lambda} \times \beta_n)\right]$, where β_n are the Boubaker polynomials [31–36] B_{4n} minimal positive roots, θ_n are given coefficients, N_0 is a given integer, $\alpha(\tilde{\lambda})$ is the normalised absorbance spectrum and $\tilde{\lambda}$ is the normalised wavelength:

$$\begin{cases} \lambda \in [\lambda_{min}, \lambda_{max}] \Leftrightarrow \tilde{\lambda} \in [0, 1] \\ \lambda_{min} = 0.3\ \mu m; \quad \lambda_{max} = 1.8\ \mu m \end{cases} \tag{3}$$

The normalised absorbance spectrum $\alpha(\tilde{\lambda})$ is deduced from the BPES by establishing a set of N experimental measured values of the transmittance–reflectance vector $(T_i(\tilde{\lambda}_i); R_i(\tilde{\lambda}_i))\big|_{i=1..N}$ versus the normalised wavelength $\tilde{\lambda}_i\big|_{i=1..N}$. Then the system (4) is set:

$$\begin{cases} R(\tilde{\lambda}) = \left[\dfrac{1}{2N_0}\displaystyle\sum_{n=1}^{N_0}\xi_n \times B_{4n}(\tilde{\lambda} \times \beta_n)\right] \\ T(\tilde{\lambda}) = \left[\dfrac{1}{2N_0}\displaystyle\sum_{n=1}^{N_0}\xi'_n \times B_{4n}(\tilde{\lambda} \times \beta_n)\right] \end{cases} \tag{4}$$

where β_n are the $4n$-Boubaker polynomials B_{4n} minimal positive roots [33–37], N_0 is a given integer and ξ_n and ξ'_n are coefficients determined through the Boubaker Polynomials Expansion Scheme (BPES).

Table 1
Relevant parameters (before and after sulfurisation).

SnO_2:F	Before sulfurisation	After light sulfurisation	After heavy sulfurisation
E_g (eV)	4.00	3.90	3.00–2.48
ψ_{AB} ($\times 10^{-12}$ m^3 s^{-1})	23.8	29.5	35.6

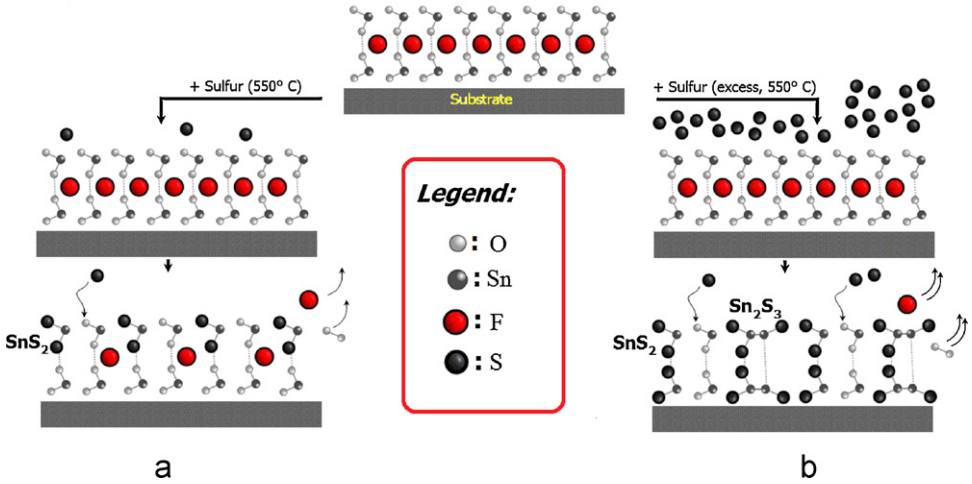

Fig. 8. Sulfuration kinetics sketch. (a) Lightly sulfured SnO_2 and (b) heavily sulfured SnO_2.

The normalised absorbance spectrum $\alpha(\tilde{\lambda})$ is deuced from the relation:

$$\alpha(\tilde{\lambda}) = \frac{1}{d\sqrt[4]{2}} \cdot \sqrt[4]{\left(\ln\frac{1-R(\tilde{\lambda})}{T(\tilde{\lambda})}\right)^4 + \left(2\ln\frac{1-R(\tilde{\lambda})}{\sqrt{T(\tilde{\lambda})}}\right)^4} \quad (5)$$

where d is the layer thickness.

The obtained value of normalised absorbance spectrum $\alpha(\tilde{\lambda})$ is a final guide to the determination of the effective absorptivity $\hat{\alpha}$ through (Eq. (2)).

The Amlouk–Boubaker opto-thermal expansivity ψ_{AB} is a thermo-physical parameter defined in precedent studies [40–43], as a 3D expansion velocity of the transmitted heat inside the material. It is expressed in $m^3\,s^{-1}$, and calculated by:

$$\psi_{AB} = \frac{D}{\hat{\alpha}} \quad (6)$$

where D is the material's thermal diffusivity [41] and $\hat{\alpha}$ is the already defined effective absorptivity (Eq. (2)).

The values of the calculated values of the Amlouk–Boubaker opto-thermal expansivity ψ_{AB}, for the different samples, are gathered in Table 1.

4. Discussion and perspectives

A very instructive study has been presented by Ramakrishna Reddy et al. [44] on the annealing temperature ranges selectiveness during the formation of Sn_xS_y binary materials. The authors have observed, in agreement with the reports of Lopez et al. [45] and Thangaraju et al. [46], that Sn–S compounds are predominant for sulfurisation temperatures superior to 300 °C. Koteeswara-Reddy et al. [47] stated similarly that Sn_xS_y films grown at high temperatures were nearly stoichiometric in nature with an elemental Sn/S ratio of 1.03. In fact, under high temperatures, the Sn–O bonds are weakened inside the structure (Fig. 8a). Under a moderate sulfur concentration S/O, substitution occurs randomly but efficiently. An excess of sulfur supply causes a deeper substitution process (Fig. 8b) resulting in big amounts of Sn_2S_3 and SnS_2 as deduced from XRD and AFM analysis.

It has been indeed reported that such binary compounds could be obtained by direct contact between metallic films and elemental sulfur [44,48–52], but a simple comparison between these routes and the mechanism using appropriate doping (i.e. Fluorine [53–60]) shows that the kinetics observed in the actual study are quite 400 times quicker.

Moreover, the optothermal study revealed an obvious enhancement of the Amlouk–Boubaker opto-thermal expansivity ψ_{AB}. In fact, after sulfurisation, a higher value of ψ_{AB} has been recorded (Table 1). Since this parameter indicates and brings together a high thermal diffusivity (hence a good heat transmittance) of the compound along with a high absorption coefficient which is required for some optical applications in thermally aggressive mediums.

5. Conclusions

In summary, we have discussed the effects of the controlled sulfurisation on as-grown SnO_2:F thin films prepared at 440 °C using a simplified and already optimized spray pyrolysis setup. Sulfurisation kinetics have been investigated through the results of several characterization techniques. It has been shown, in concordance with the recent literature, that the mechanism is drastically enhanced by the presence of the doping agent (i.e. fluorine), and that excesses of sulfur in the reactive medium leads to an interesting mixture of Sn_xS_y binary compounds (namely, SnS_2 and Sn_2S_3). Additional optical and optothermal analyses revealed a loss of bandgap (down to 18%) along with a drastic increase of the Amlouk–Boubaker opto-thermal expansivity ψ_{AB}. These two features make the proposed sulfurisation process promising for opto-electronic and solar energy devices, particularly those needing appropriate heat diffusion means.

Nevertheless, it has been noted, by colleagues from collaborating laboratories, that the electrical resistivity of the yielded films was abnormally high. A vacuum heat treatment under inert atmosphere is being carried out in order to enhance the obtained layers electrical behavior.

References

[1] S.K. Panda, A. Antonakos, E. Liarokapis, S. Bhattacharya, S. Chaudhuri, Mater. Res. Bull. 42 (2007) 576.
[2] S. Acharya, O.N. Srivastava, Phys. Stat. Sol. A 65 (1981) 717.
[3] Y. Saiga, K. Suekuni, S.K. Deng, T. Yamamoto, Y. Kono, N. Ohya, T. Takabatake, J. Alloys Compd. 507 (2010) 1.
[4] N.G. Deshpande, A.A. Sagade, Y.G. Gudage, C.D. Lokhande, R. Sharma, J. Alloys Compd. 436 (2007) 421.
[5] S.K. Arora, D.H. Patel, M.K. Agarwal, Mater. Chem. Phys. 45 (1996) 63.
[6] A. Akkari, C. Guasch, N. Kamoun-Turki, J. Alloys Compd. 490 (2010) 180.
[7] G.H. Yue, W. Wang, L.S. Wang, X. Wang, P.X. Yan, Y. Chen, D.L. Peng, J. Alloys Compd. 474 (2010) 445.
[8] A.S. Khomane, J. Alloys Compd. 506 (2010) 849.
[9] P.A. Chate, P.P. Hankare, D.J. Sathe, J. Alloys Compd. 505 (2010) 140.
[10] C. Khélia, K. Boubaker, T. Ben Nasrallah, M. Amlouk, S. Belgacem, F. Saadallah, N. Yacoubi, J. Cryst. Growth 311 (4) (2009) 1032–1035.
[11] M. Khadraoui, N. Benramdane, C. Mathieu, A. Bouzidi, R. Miloua, Z. Kebbab, K. Sahraoui, R. Desfeux, Solid State Commun. 150 (2010) 297.
[12] T.H. Sajeesh, R. Anita, C. Warrier, K.P. Sudha Kartha, Vijayakumar, Thin Solid Films 518 (2010) 4370.
[13] M. Cruz, J. Morales, J.P. Espinos, J. Sanz, J. Solid State Chem. 175 (2003) 359.
[14] T.G. Hibbert, M.F. Mahon, K.C. Molloy, L.S. Price, I.P. Parkin, J. Mater. Chem. 11 (2001) 469.
[15] I.P. Parkin, L.S. Price, T.G. Hibbert, K.C. Molloy, J. Mater. Chem. 11 (2001) 1486.
[16] R. Schlaf, N.R. Armstrong, B.A. Parkinson, C. Pettenkofer, W. Jaegermann, Surf. Sci. 385 (1997) 1.
[17] N.G. Deshpande, A.A. Sagade, Y.G. Gudage, C.D. Lokhande, Ramphal Sharma, J. Alloys Compd. 436 (2007) 421.
[18] B. Ghosh, M. Das, P. Banerjee, S. Das, Appl. Surf. Sci. 254 (2008) 6436.
[19] R.D. Engelken, H.E. Mc Coud, C. Lee, M. Slayton, H. Ghoreishi, J. Electrochem. Soc. 134 (1987) 2696.
[20] A. Sánchez-Juárez, A. Tiburcio-Silver, A. Ortiz, Thin Solid Films 480 (2005) 452.
[21] S. Belgacem, M. Amlouk, R. Bennaceur, Rev. Phys. 25 (1990) 1213–1233.
[22] J.C.P.D.S - International Center for diffraction data 88-0287 (2000).
[23] B.D. Cullity, Elements of X-ray Diffraction, Addisson–Wesley Publishing Co., 1956, p. 98.
[24] L. Bhira, M. Amlouk, S. Belgacem, R. Bennaceur, D. Barjon, Phys. Stat. Sol. A 165 (1998) 141.
[25] S. Belgacem, R. Bennaceur, Rev. Phys. Appl. 24 (1990) 1245.
[26] E.J. Johson, Semiconductors and Semimetals. 3. Optical Properties of III–V Compounds, Academic Press, NY, 1967.
[27] S.K. Panda, A. Antonakos, E. Liarokapis, S. Bhattacharya, S. Chaudhuri, Mater. Res. Bull. 42 (2007) 576–583.
[28] H. Ben Hadj Salah, H. Bouzouita, B. Rezig, Thin Solid Films 480 (2005) 439.
[29] K.B. Ben Mahmoud, M. Amlouk, Mater. Lett. 63 (2009) 991–999.
[30] S. Lazzez, K.B. Ben Mahmoud, S. Abroug, F. Saadallah, M. Amlouk, Curr. Appl. Phys. 9 (2009) 1129–1134.
[31] B. Dubey, T.G. Zhao, M. Jonsson, H. Rahmanov, J. Theor. Biol. 264 (2010) 154.
[32] D.H. Zhang, F.W. Li, Ir. J. Appl. Phys. Lett. 2 (2009) 25.
[33] T.G. Zhao, L. Naing, W.X. Yue, Mater. Zametki 87 (2) (2010) 175.
[34] A. Yildirim, S.T. Mohyud-Din, D.H. Zhang, Comp. Math. Appl. 59 (2010) 2473.
[35] A. Belhadj, J. Bessrour, M. Bouhafs, L. Barrallier, J. Therm. Anal. Calorim. 97 (2009) 911.
[36] S. Tabatabaei, T. Zhao, O. Awojoyogbe, F. Moses, Heat Mass Transf. 45 (2009) 1247.
[37] S. Fridjine, M. Amlouk, Mod. Phys. Lett. B 23 (2009) 2179.
[38] O.D. Oyodum, O.B. Awojoyogbe, M. Dada, J. Magnuson, Eur. Phys. J. Appl. Phys. 46 (2009) 21201.
[39] A. Belhadj, O. Onyango, N. Rozibaeva, J. Thermophys. Heat Transf. 23 (2009) 639.
[40] S. Lazzez, K.B. Ben Mahmoud, S. Abroug, F. Saadallah, M. Amlouk, Curr. Appl. Phys. 9 (2009) 1129.
[41] K.B. Ben Mahmoud, M. Amlouk, Mater. Lett. 63 (2009) 991.
[42] J. Ghanouchi, H. Labiadh, K. Boubaker, Int. J. Heat Techn. 26 (2008) 49.
[43] S. Slama, M. Bouhafs, K.B. Ben Mahmoud, Int. J. Heat Techn. 26 (2008) 141.
[44] K.T. Ramakrishna Reddy, P. Purandhara Reddy, P.K. Datta, R.W. Miles, Thin Solid Films 403–404 (2002) 116.
[45] S. Lopez, A. Ortiz, Semicond. Sci. Technol. 9 (1994) 2130.
[46] B. Thangaraju, P. Kaliannan, J. Phys. D: Appl. Phys. 33 (2000) 1054.
[47] N. Koteeswara Reddy, K.T. Ramakrishna Reddy, Physica B 368 (2005) 25.

[48] P. Pramanik, P.K. Basu, S. Biswas, Thin Solid Films 150 (1987) 267.
[49] M.T.S. Nair, P.K. Nair, Semicond. Sci. Technol. 6 (1991) 132.
[50] K. Mishra, K. Rajeshwar, A. Weiss, M. Murley, R.D. Engelken, M. Slayton, H.E. McCloud, J. Electrochem. Soc. 136 (1989) 1915.
[51] M. Sharon, P. Veluchamy, C. Natarajan, D. Kumar, Electrochim. Acta 36 (1991) 1107.
[52] B. Subramanian, C. Sanjeeviraja, M. Jayachandran, Mater. Chem. Phys. 71 (2001) 40.
[53] E. Elangovan, K. Ramamurthi, J. Optoelectron. Adv. Mater. 5 (2003) 45.
[54] G. Gordillo, L.C. Moreno, W. Cruz, P. Teheran, Thin Solid Films 252 (1994) 61.
[55] P.K. Nair, M.T.S. Nair, J. Campos, J. Electrochem. Soc. 140 (1993) 539.
[56] S. Kulaszewicz, Thin Solid Films 74 (1980) 211.
[57] S. Kulaszewicz, I. Lasocka, Cz. Michalski, Thin Solid Films 55 (1978) 283.
[58] J.F. Jordan, S.P. Albright, Sol. Cells 23 (1988) 107.
[59] R. Acosta, E.P. Zironi, E. Montoya, W. Estrada, Thin Solid Films 288 (1996) 1.
[60] K. Nomura, Y. Ujihira, S.S. Sharma, A. Fueda, T. Murakami, J. Mater. Sci. 24 (1989) 937.